Ultraviolet photolysis and proton irradiation of astrophysical ice analogs containing hydrogen cyanide

ARTICLE *in* ICARUS · JULY 2004

Impact Factor: 3.04 · DOI: 10.1016/j.icarus.2004.02.005

Available online at www.sciencedirect.com
SCIENCE DIRECT®
Icarus 170 (2004) 202–213
ICARUS
www.elsevier.com/locate/icarus

Ultraviolet photolysis and proton irradiation of astrophysical ice analogs containing hydrogen cyanide

P.A. Gerakines,[a,*] M.H. Moore,[b] and R.L. Hudson[c]

[a] *Astro- and Solar-System Physics Program, Department of Physics, University of Alabama at Birmingham, 1300 University Blvd, CH 310, Birmingham, AL 35294-1170, USA*
[b] *Astrochemistry Branch, Code 691, NASA/Goddard Space Flight Center, Greenbelt, MD 20771, USA*
[c] *Department of Chemistry, Eckerd College, St. Petersburg, FL 33733, USA*

Received 26 September 2003; revised 21 January 2004
Available online 1 April 2004

Abstract

Hydrogen cyanide (HCN) has been identified in the gas phase of the interstellar medium as well as in the comae of several comets. Terrestrially, HCN is a key component in the synthesis of biologically important molecules such as amino acids. In this paper, we report the results of low-temperature (18 K) ice energetic processing experiments involving pure HCN and mixtures of HCN with H_2O and NH_3. Ice films, 0.1 to several microns in thickness, were exposed to either ultraviolet photons (110–250 nm) or 0.8-MeV protons to simulate the effects of space environments. Observed products include HCNO (isocyanic acid), NH_4^+ (ammonium ion), CN^- (cyanide ion), OCN^- (cyanate ion), $HCONH_2$ (formamide), and species spectrally similar to HCN polymers. Product formation rates and HCN destruction rates were determined where possible. Results are discussed in terms of astrophysical situations in the ISM and the Solar System where HCN would likely play an important role in prebiotic chemistry. These results imply that if HCN is present in icy mixtures representative of the ISM or in comets, it will be quickly converted into other species in energetic environments; pure HCN seems to be polymerized by incident radiation.

Keywords: Ices; Comets, composition; Radiation chemistry; Photochemistry; Spectroscopy

1. Introduction

Hydrogen cyanide (HCN) has been identified in the gas phase of the interstellar medium (ISM; e.g., Snyder and Buhl, 1971; Boonman et al., 2001) as well as in the comae of several comets (e.g., Ip et al., 1990; Bockelée-Morvan et al., 1994; Magee-Sauer et al., 1999). Although not yet observed above the detection limits of the infrared absorption spectra of interstellar ices, HCN is thought to be a native component of cometary ices (in either monomeric or polymeric form), and not a product of reactions in the coma after sublimation (e.g., Magee-Sauer et al., 1999). Potentially, the observed cometary HCN could originate in interstellar ices. That being the case, HCN or its polymers could potentially play interesting roles in the energetic processing of both interstellar and cometary ices.

Terrestrially, HCN is a key component in the synthesis of biologically important molecules such as amino acids (e.g., Oro et al., 1992). Since Earth formed in a region of the Solar nebula with only sparse amounts of low-molecular-weight materials, a current hypothesis purports that cometary impacts delivered large amounts of volatile and organic materials to the young, cooling Earth (Chyba et al., 1994). It is therefore important to study the energetic processing—such as UV photolysis and particle bombardment[1]—of cometary materials in order to increase the understanding of the original reservoir of organic materials for Earth and the other planets. Based on observations of cometary comae, these materials should include icy mixtures that contain HCN.

Other possible indirect clues to the significance of HCN chemistry in comets were proposed by Matthews and Ludicky (1986), who suggested that the low albedo of the nu-

* Corresponding author. Fax: 205-934-8042.
E-mail address: gerak@uab.edu (P.A. Gerakines).

[1] Hereafter, UV photolysis and particle bombardment will be denoted simply as "photolysis" and "irradiation," respectively.

0019-1035/$ – see front matter
doi:10.1016/j.icarus.2004.02.005

cleus of Comet Halley could be due to HCN polymeric materials. This idea was expanded by Rettig et al. (1992), who postulated that cometary outbursts could be due to the explosive polymerization of HCN in cometary nuclei. Particles detected by the Giotto spacecraft during its flight through the coma of Comet Halley were found to be composed largely of the elements C, H, O, and N ("CHON particles"; Kissel, 1986). This suggests that materials representative of hydrolyzed HCN polymers (a form of tholin, which itself is essentially a nitrile-containing heteropolymer; see, e.g., Khare et al., 1994) may exist in the dust of comets.

In this paper, we report the results of ice processing experiments involving pure HCN and mixtures of HCN with H_2O and NH_3. H_2O is 5 to 10 times more abundant than the next largest component of both interstellar and cometary ices (e.g., Gibb et al., 2000). The mixture H_2O + HCN, with other mostly minor components, thus represents the majority of ice environments experienced by HCN in astrophysical situations. The HCN observed in the comae of comets is either released from the nuclear ices as they sublime, or is formed by decomposition of a polymer or oligamer of HCN (Magee-Sauer et al., 1999). Nonetheless, if HCN or a related polymeric form is a component of cometary ices before sublimation, an appropriate analog should be water-dominated.

NH_3 is also present in astrophysical ices in moderate abundance. In the ISM, its detection has been somewhat clouded by the strong, overlapping IR spectral features of interstellar H_2O and silicates, but some observations to date indicate that NH_3 may exist at concentrations as high as 10–20% relative to H_2O in several lines of sight (e.g., Gibb et al., 2001). In the comae of comets, the abundance of NH_3 has been observed at about 0.1–0.3% relative to H_2O, with a similar abundance inferred for the cometary ice (e.g., Mumma et al., 1993). Since NH_3 is a base and HCN is an acid, interesting reactions may occur that could have implications for the chemistry of astrophysical ices.

Published radiolysis studies of aqueous solutions of HCN (Draganić et al., 1973; Büchler et al., 1976; Negrón-Mendoza et al., 1983) show that a large variety of organic products form, including aldehydes (such as H_2CO), ketones (such as acetone), and carboxylic acids (such as oxalic, succinic, or glutaric acid). The fruitful nature of the aqueous HCN radiolysis implies that HCN contained in solid matrices with H_2O may also yield a complex chemistry involving prebiotic molecules. Recent laboratory work by Bernstein et al. (2002) has shown that the presence of HCN in icy materials such as cometary or interstellar H_2O and NH_3 should lead to the formation of simple amino acids through processing by ultraviolet photons. These authors showed that an HCN-containing laboratory ice analog (a four-component mixture with the composition of $H_2O + CH_3OH + NH_3 +$ HCN in the ratio of 100:10:5:5) forms simple racemic amino acids when exposed to vacuum-UV photons.

We have studied the IR spectra of ice samples at 18 K composed of pure HCN, H_2O + HCN (5:1), NH_3 + HCN (5:1), or $H_2O + NH_3$ + HCN (5:5:1), during energetic processing. These mixtures were not chosen to model the actual ice composition in the ISM or in comets, but because they clearly demonstrate the chemical behavior of HCN in various ice environments of interest. As far as we are aware, this is the first laboratory study of HCN-bearing ices to examine the effects of both UV photolysis and particle irradiation. Ices were exposed to either vacuum-UV photolysis or irradiation by 0.8-MeV protons. Product formation rates and HCN destruction rates were determined. We relate our results to astrophysical situations in the ISM and the Solar System where HCN would likely play an important role in prebiotic chemistry.

2. Experiment

The equipment and ice sample preparation procedures in the Cosmic Ice Laboratory at NASA's Goddard Space Flight Center have been described in detail elsewhere by, for example, Hudson and Moore (1995) and Gerakines et al. (2000). In summary, ice samples in the form of films ranging in thickness from about 0.1 to 5 μm are created on an aluminum mirror substrate that may be cooled to temperatures of 10–20 K, with 18 K as the lowest temperature used in these experiments. The temperature of the substrate may be controlled up to 300 K using a resistive heater element and thermocouple. The thicknesses of the ice samples are measured by monitoring the evolution of interference fringes of laser light reflected from the substrate during the ice film's growth. The substrate rotates such that it may face a port to either the mid-IR spectrometer (Mattson Instruments Polaris FTIR) for spectroscopic analysis (from 5000–400 cm^{-1}, with a resolution of 4 cm^{-1}), the 0.8-MeV proton beam produced by a Van de Graaff accelerator for irradiations, or the output of a microwave-discharged hydrogen flow lamp (Opthos Instruments) for ultraviolet photolysis.

The spectrum of the radiation emitted by the UV lamp at NASA/GSFC is shown in Fig. 1, and the techniques of its recent calibration are described in detail by Cottin et al. (2003). It produces vacuum-UV photons with wavelengths longer than 100 nm (determined by the cut-off limits of the LiF window used to separate it from the vacuum system), and in the spectral range where H_2O ice strongly absorbs vacuum UV radiation ($\lambda < 180$ nm; e.g., Dressler and Schnepp, 1960), the average output energy is approximately 7.9 eV ($\lambda = 157$ nm) in the range from $\lambda = 100$–180 nm as determined from the output spectrum as shown in Fig. 1. Note that this value is lower than the 10.2 eV for Lyman-α photons that is typically assumed for these lamps.[2] The total

[2] In light of these recent UV lamp calibrations, and since this lamp's set-up is nearly identical to that of other laboratories where UV lamp fluxes have been heretofore based on assumed parameters (e.g., Gerakines et al., 1996, 2000, and many others in various laboratories), it may be worth reconsidering the reported parameters (such as formation and destruction rates) in terms of the data presented here and by Cottin et al. (2003).

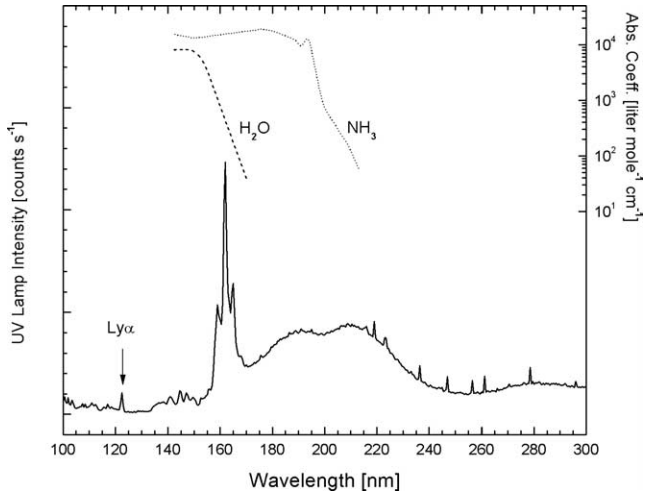

Fig. 1. Spectrum, from 100 to 300 nm, of the output of the vacuum-ultraviolet photolysis lamp used in the Cosmic Ice Laboratory at NASA/GSFC. The wavelength of Lyman-α photons (121.6 nm) is indicated. The molar absorption coefficients of H_2O (dashed line) and NH_3 (dotted line) solids at 77 K (from Dressler and Schnepp, 1960) are also shown.

photon flux of 5.3×10^{14} photons $cm^{-2}\,s^{-1}$ was measured at the location of the aluminum substrate inside the vacuum system, and (multiplying by the value for $\langle E \rangle$ of 7.9 eV) corresponds to a total energy flux of 4.2×10^{15} eV $cm^{-2}\,s^{-1}$.

Energy doses for the processing radiation (0.8-MeV protons or vacuum-UV photons) in this report are expressed in the units of eV cm^{-2} to facilitate comparisons between irradiation and photolysis experiments and for simplicity in the calculation of formation and destruction rates (described below). The energy dose in an irradiation experiment is derived from the measured integrated current that passes through the sample, the ice sample thickness (measured during deposit using reflected laser interference fringes), the ice sample's stopping power, and the ice sample's assumed mass density. For a photolysis experiment, the energy dose is calculated from the UV lamp's known photon flux, the average photon energy emitted by the lamp (measured from the spectrum in Fig. 1), the total UV exposure time, and the assumption that all photons are absorbed in the ice sample, which is generally true for H_2O ice thicker than about 1 μm (although they are not uniformly absorbed throughout the entire sample). See the discussions by Gerakines et al. (2000, 2001) and Gerakines and Moore (2001) for a more detailed background into comparisons between the results of ice irradiation and photolysis experiments.

The HCN gas used in these experiments was synthesized in a laboratory vacuum manifold by reactions of KCN (potassium cyanide) and $CH_3(CH_2)_{16}COOH$ (stearic acid) powders in approximately equal molar ratio. The powder mixture was heated to 350 K, in order to melt the stearic acid and drive its reaction with KCN, and held at that temperature until the reaction ceased. The gases that were released during the heating, namely HCN and CO_2, were collected in a bulb that was cooled to 77 K by immersion in liquid N_2. The CO_2 was pumped away by replacing the liquid N_2 with an acetone slush bath at 178 K. The HCN remained frozen in the bulb. Although this final step was repeated before each experiment to purify the HCN gas, CO_2 contamination is present in some of the samples and is visible in some of the mid-IR spectra presented in the next section.

In the following section, we describe the results of experiments involving vapor-condensed samples at 18 K composed of pure HCN, HCN mixed with either H_2O (H_2O + HCN, 5:1) or NH_3 (NH_3 + HCN, 5:1), and HCN mixed with both H_2O and NH_3 (H_2O + NH_3 + HCN, 5:5:1). Since HCN is highly soluble in H_2O and since NH_3 and HCN react in the gas phase, it was necessary to keep these components physically separated before the time of sample condensation. The mixed solid sample was created by simultaneously leaking each gas through a separate line into the vacuum chamber, to a point in front of the cold Al mirror. Appropriate flow rates for each gas component were determined ahead of time, by determining the correlation of the pressure decrease in the gas bulb to the growth of a resulting ice film. Desired compositions for the mixed samples were then obtained by allowing the pressure in each gas component's bulb to drop at the proper rate during the sample condensation. Final ice compositions were determined by IR spectroscopy of the resulting samples. Although this method does not guarantee perfect homogeneity of mixing, it has been shown to create samples that are spectroscopically identical in the mid IR to those originating from pre-mixed gases (Gerakines et al., 1995).

3. Results

In this section, we describe the spectroscopic results of the irradiation and photolysis experiments on pure HCN, H_2O + HCN (5:1), NH_3 + HCN (5:1), and H_2O + NH_3 + HCN (5:1:1) at 18 K, and quantify some rates for HCN destruction and the formation of certain products.

3.1. Pure HCN

The IR spectra of three 18 K pure HCN samples at different thicknesses (0.4, 1.0, and 2.2 μm) are shown in Fig. 2. The four strongest absorption features appear at 3100, 2102, 1626, and 823 cm^{-1}. By measuring the total absorption for pure HCN samples of different thicknesses, we have calculated the IR band strength for the C–N stretching feature of pure HCN (2102 cm^{-1}) at 18 K. Our result is in agreement with the value of 5.1×10^{-18} cm molecule^{-1} as measured by Bernstein et al. (1997) for HCN as a constituent of H_2O + HCN ice samples at low temperature.

We have performed both irradiation and photolysis experiments on pure HCN samples at low temperature. Figures 3a and 3b display the spectrum of a pure HCN ice sample at 18 K before and after various stages of irradiation with 0.8-MeV protons. After processing, spectral fea-

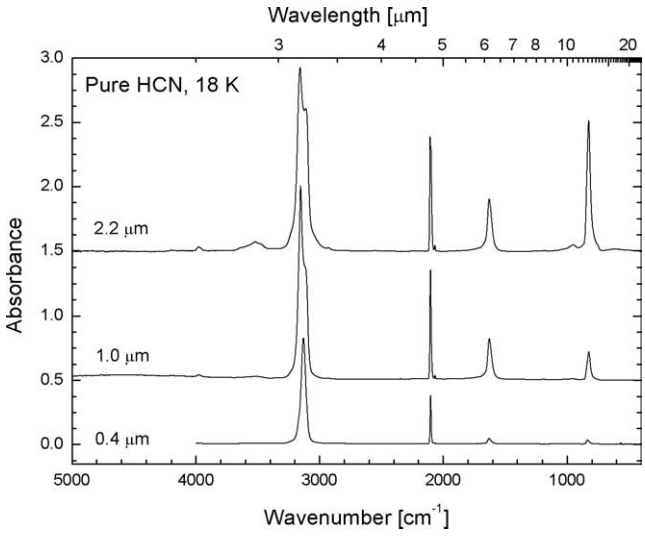

Fig. 2. IR spectra from 5000 to 400 cm^{-1} (2.0–25 μm) of pure HCN samples at three thicknesses. From top to bottom: 2.2, 1.0, and 0.4 μm. Spectra have been offset for comparison purposes.

tures appear at 2217, 1455, and 1079 cm^{-1}, consistent with the growth of an HCN dimer such as *N*-cyanomethanimine (Evans et al., 1991) or other oligamers of HCN. Other strong absorptions, which remain unidentified, were observed after irradiation at 2303, 2143, 1720, 1345, and 1122 cm^{-1}. The growth of a feature due to the ionic group CN^- is suspected near 2090 cm^{-1}, represented in our spectra as the growth of a feature underneath the HCN feature, resulting in the gradual broadening and redshift of the HCN stretching feature at 2100 cm^{-1} during irradiation (see Fig. 3b). IR spectra of the pure HCN samples that were processed by UV photolysis reveal no major differences to those that were irradiated, as displayed in Fig. 3c. The absorption feature of CO_2 appears to grow with energy dose in both sets of experiments, indicating that there is some oxygen-bearing impurity in the vacuum system during the experiment. It is unlikely that the unidentified features named above could also be due to this impurity, since the amount of CO_2 produced in each experiment does not appear to correlate with their growth.

3.2. $H_2O + HCN$

We have studied the irradiation and photolysis of samples containing H_2O + HCN (5:1 or 9:1) at 18 K. Figure 4a contains the complete 5000–500 cm^{-1} (2–20 μm) spectrum of a 5.5-μm thick H_2O + HCN (5:1) sample at 18 K before and after irradiation to various energy doses. Figure 4b contains enlargements of the 2400–2000 cm^{-1} (4.2–5 μm) region of these spectra. Figure 4c contains the 2400–2000 cm^{-1} (4.2–5 μm) region of a photolyzed H_2O + HCN (9:1) ice sample at 18 K. As most HCN spectral features overlap with those of H_2O, only the C–N stretching feature is apparent at 2092 cm^{-1} (4.78 μm) with a FWHM of 20 cm^{-1}. A weak feature at 2342 cm^{-1} (4.27 μm) is also apparent, due to a

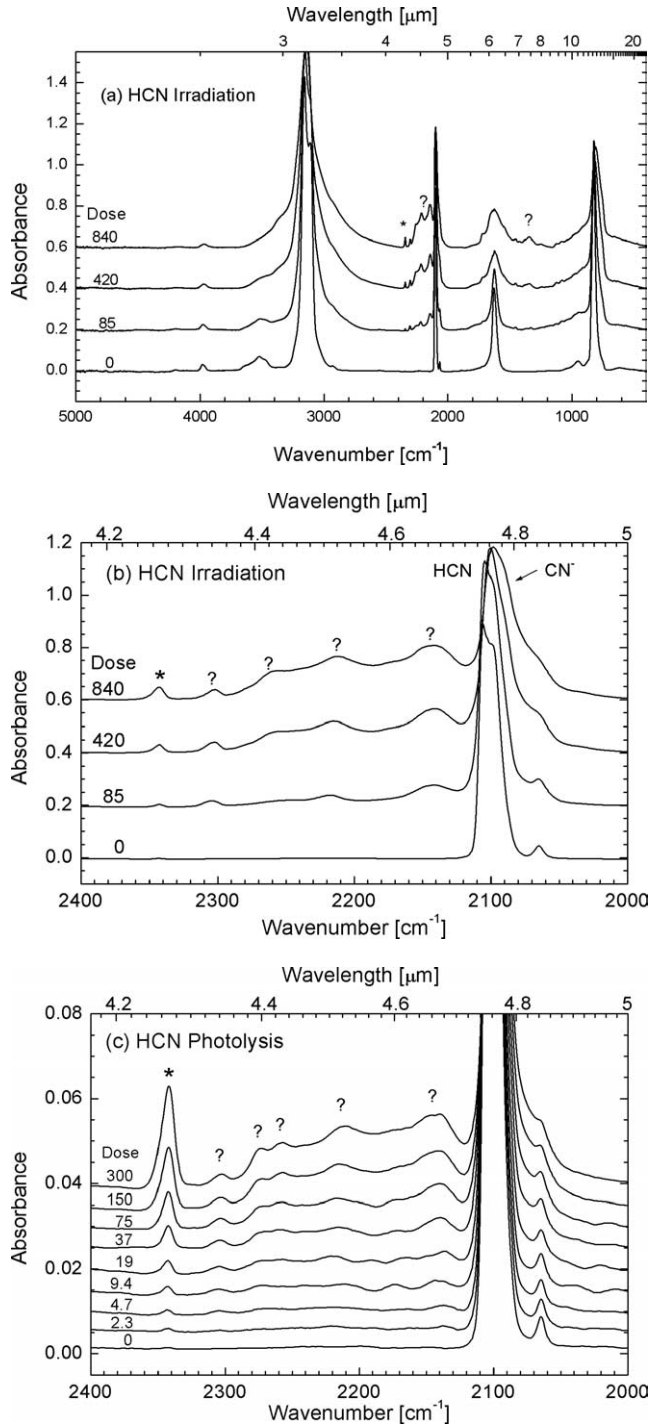

Fig. 3. (a) IR spectrum from 5000 to 400 cm^{-1} (2.0–25 μm) of pure HCN (2.2 μm thick) processed at 18 K by irradiation. (b) 2400–2000 cm^{-1} (4.17–5.0 μm) region of the irradiated HCN sample for comparison to (c) IR spectrum of UV photolyzed pure HCN (0.4 μm in thickness). Doses are in units of 10^{17} eV cm^{-2}. The feature marked by an asterisk is due to CO_2 and is a product of contamination in the sample. Unidentified features are labeled with a question mark.

small amount of CO_2 remaining in the HCN gas bulb after purification (∼ 0.1% relative to HCN; see Section 2).

After processing, a feature at 2169 cm^{-1} (4.61 μm) with a width of 31 cm^{-1} is observed, matching well the

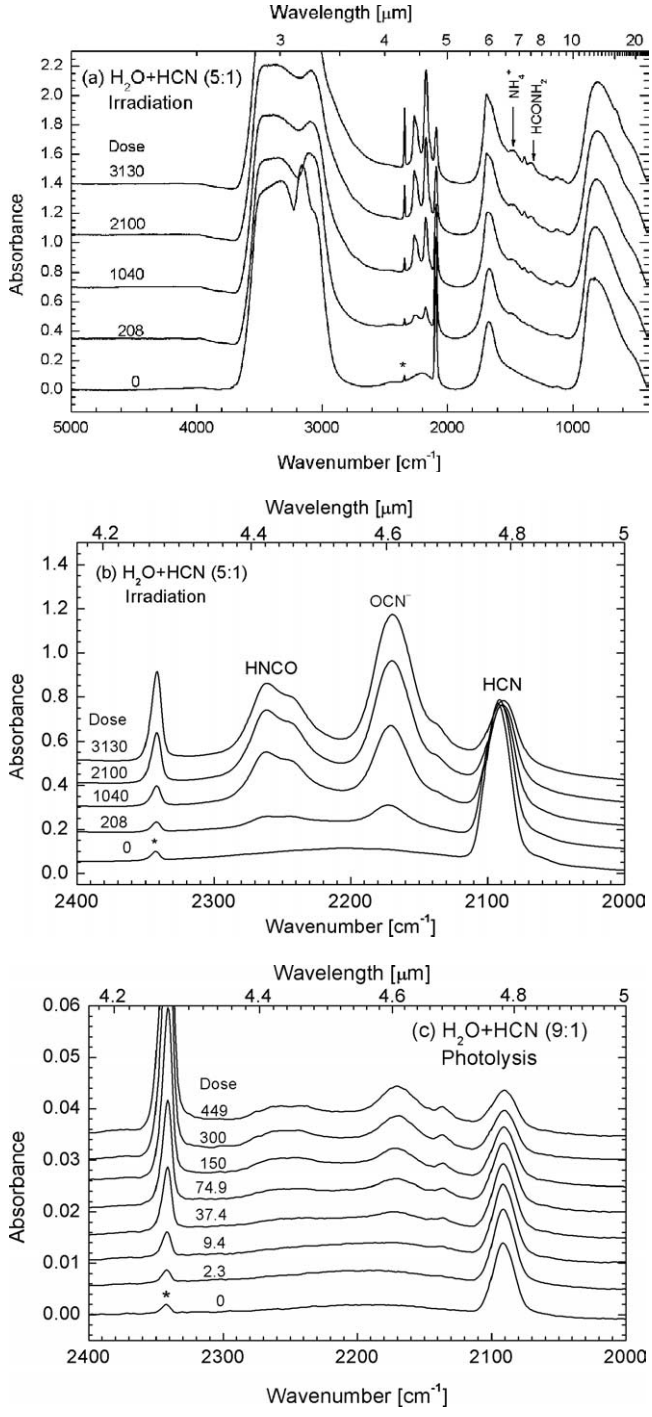

Fig. 4. (a) IR spectrum from 5000 to 400 cm^{-1} (2.0–25 μm) of an H_2O + HCN (5:1) ice sample processed at 18 K by irradiation. (b) 2400–2000 cm^{-1} region of the irradiated H_2O + HCN (5:1) sample for comparison to (c) an H_2O + HCN (9:1) ice sample processed by photolysis at 18 K. Doses are in units of 10^{17} eV cm^{-2}. The absorption features of CO_2 in the initial ice deposits are marked by asterisks.

OCN^- anion seen in a variety of processed ices, such as $H_2O + NH_3 + CO$ (Hudson et al., 2001). The feature in both the irradiated and photolyzed ice samples that falls at 2268 cm^{-1} (4.41 μm) with a width of 40 cm^{-1} is indicative of isocyanic acid (HNCO; see Khanna et al., 2002). The CO_2 absorption feature at 2342 cm^{-1} also grows with processing. Features in the 1800–1000 cm^{-1} region suggest the presence of the NH_4^+ cation at 1470 cm^{-1} (6.80 μm), and formamide ($HCONH_2$) at both 1686 cm^{-1} (5.93 μm) and 1386 cm^{-1} (7.22 μm). Formamide and NH_4^+ were both identified in the IR spectrum of NH_3 + CO after photolysis by, e.g., Demyk et al. (1998). It may be worth noting that the processed H_2O + HCN ice spectra also bear resemblance to those of processed NH_3 + CO (1:1) by Hudson et al. (2001).

3.3. NH_3 + HCN

The IR spectrum of an NH_3 + HCN (5:1) ice sample condensed at 18 K is shown in Fig. 5. A strong feature at 1479 cm^{-1} (6.76 μm), due neither to NH_3 nor HCN is observed upon the initial ice deposit. We observed this feature in the spectrum of every ice sample that contained both NH_3 and HCN (irrespective of the other components). The peak position of this feature is consistent with the NH_4^+ cation.

Two tests were performed to confirm the assignment of this feature to NH_4^+. The first is that after two slow annealing cycles to 140–150 K (at a rate of about 2 to 5 K min^{-1}), the IR spectrum of the NH_3 + HCN sample (Fig. 5) was found to be identical to that of crystalline ammonium cyanide (NH_4CN) as measured by Clutter and Thompson (1969) (topmost spectrum in Fig. 5). In their experiments, NH_4CN was produced by depositing a NH_3 + HCN (1:1) gas mixture at 125 K. In ours, the original 18 K ice was annealed in order to create a crystalline sample. Spectral changes that crystallize the NH_4CN are irreversible, and re-cooling to 18 K has no effect on the spectrum once crystallization is complete in the sample. The second piece of evidence comes from two separate experiments in which NH_3 + HCN (1:1) and $^{15}NH_3$ + HCN (1:1) mixtures were deposited at 18 K, annealed by slow heating to 150 K, and then re-cooled to 18 K. As a result, the NH_4^+ feature in the $^{14}NH_3$ deposit was observed at 1436 cm^{-1}, and the corresponding feature in the $^{15}NH_3$ deposit was observed at 1432 cm^{-1}, for a total shift of 4 cm^{-1}. Some uncertainty exists in the precision of our measurement, since the observed isotopic shift is very close to the spectrometer's resolution, but it is in approximate agreement with the results of Morgan et al. (1957), who observed the isotopic shift of NH_4^+ between NH_4Cl and $^{15}NH_4Cl$ at 83 K to be 5 cm^{-1}. This further indicates that the carrier in our 18 K samples is NH_4^+.

The formation of ammonium cyanide salt would suggest that an acid-base reaction occurs between NH_3 and HCN when the two species are co-deposited, even at the low temperature of 18 K. Since these ice samples were created by simultaneously depositing the HCN and NH_3 components from separate gas lines and were not mixed until they were released into the vacuum system just in front of the cold substrate, we consider it unlikely that this reaction took place in the gas phase. A more likely explanation is that it is driven by the heat of condensation released when the molecules adhere to the substrate.

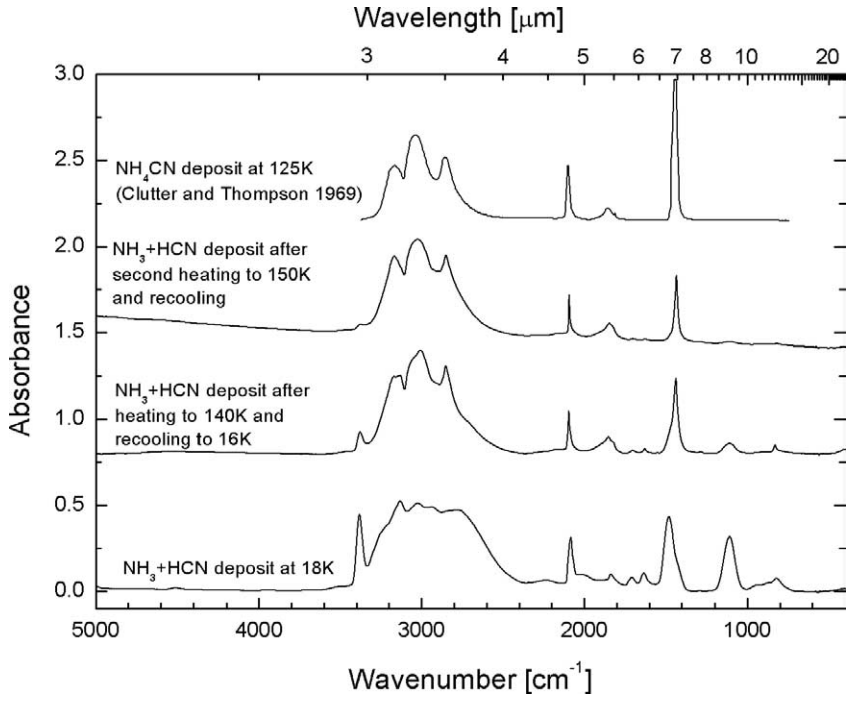

Fig. 5. Annealing of $NH_3 + HCN$ ice sample to make NH_4CN, compared to NH_4CN from Clutter and Thompson (1969).

Figure 6 shows the 2400–2000 cm^{-1} and 1800–1000 cm^{-1} regions of the $NH_3 + HCN$ (5:1) ice samples for both the irradiation (Fig. 6a) and photolysis experiments (Fig. 6b). Before processing, the feature of HCN at 2100 cm^{-1} appears with an overlapping feature centered near 2080 cm^{-1}. Due to our confidence in identifying the 1436 cm^{-1} with NH_4^+, and since NH_3 and HCN react to form NH_4CN (as shown by the deposits already described), the 2080 cm^{-1} feature is likely due to the CN^- anion. The 2100 cm^{-1} feature grows and broadens with respect to the 2080 cm^{-1} peak during irradiation (Fig. 6a). The feature of NH_4^+ at 1436 cm^{-1} also weakens slightly with irradiation dose. Features appearing after irradiation (except for the small amount of CO_2 present at 2340 cm^{-1} due to impurities in the gas mixture and the vacuum system) fall at 2205, 2159, and 1347 cm^{-1} (Fig. 6a). The position of the 1347 cm^{-1} feature corresponds to one of the strongest features (the ν_6 fundamental) of the methylenimine molecule (H_2CNH) as reported by Jacox and Milligan (1975). The other strong H_2CNH features they report fall near 1066, 1129, 1452, and 1639 cm^{-1}, but these are likely hidden by the strong features of NH_3, HCN, and NH_4^+ in our experiments. The peak positions and widths of the features as 2205 and 2159 cm^{-1} (with widths of 19 and 20 cm^{-1}, respectively) are well matched by those of dicyandiamide [$NHC(NH_2)NHCN$] in an H_2O matrix at 12 K (2204 and 2159.5 cm^{-1}, with equal widths of 21 cm^{-1}) as reported by Bernstein et al. (1997).

The spectral features that arise in the photolysis of $NH_3 +$ HCN (5:1) (Fig. 6b) are similar in character to those in the irradiation experiments. However, in this experiment, the 2080 cm^{-1} feature due to CN^- appears as a shoulder to the much stronger 2100 cm^{-1} feature of HCN in the initial ice sample, and it is the 2080 cm^{-1} feature that grows with respect to the 2100 cm^{-1} feature during processing. There is no apparent change in the feature of NH_4^+ during photolysis. It would appear that the relative strengths of these features in the initial ice samples depend on the conditions under which the sample was condensed (e.g., samples intended for photolysis are much thinner than those for irradiation).

As in the $NH_3 + HCN$ (5:1) irradiation experiment, a feature appears after processing (in this case, after 4 min of UV photolysis) near 1342 cm^{-1}, which is likely due to H_2CNH (see Fig. 6b). Features assigned to dicyandiamide in the irradiation experiment appear after photolysis as well, but they each appear at a slightly higher wavenumber, at 2211 and 2170 cm^{-1}. As before, contamination due to a small amount of CO_2 is evidenced by the CO_2 stretching feature near 2340 cm^{-1} and (in the photolysis case only) by the growth during processing of a feature due to the carbonyl (–C=O) stretching mode at 1723 cm^{-1}.

3.4. $H_2O + NH_3 + HCN$

The mixture $H_2O + NH_3 + HCN$ (in the approximate ratio of 5:5:1) was also investigated. Due to the fact that these components interact in the gas phase, they could not be pre-mixed, and were deposited according to the relative rates of pressure decrease in separate bulbs (as described in Section 2). Using this method of sample deposit, it was not possible to obtain an appropriately thin sample for photolysis experiments, and thus only irradiation experiments were performed for this ice mixture. The similarities between the effects of photolysis and irradiation in the experiments described previously suggest that there would be few differ-

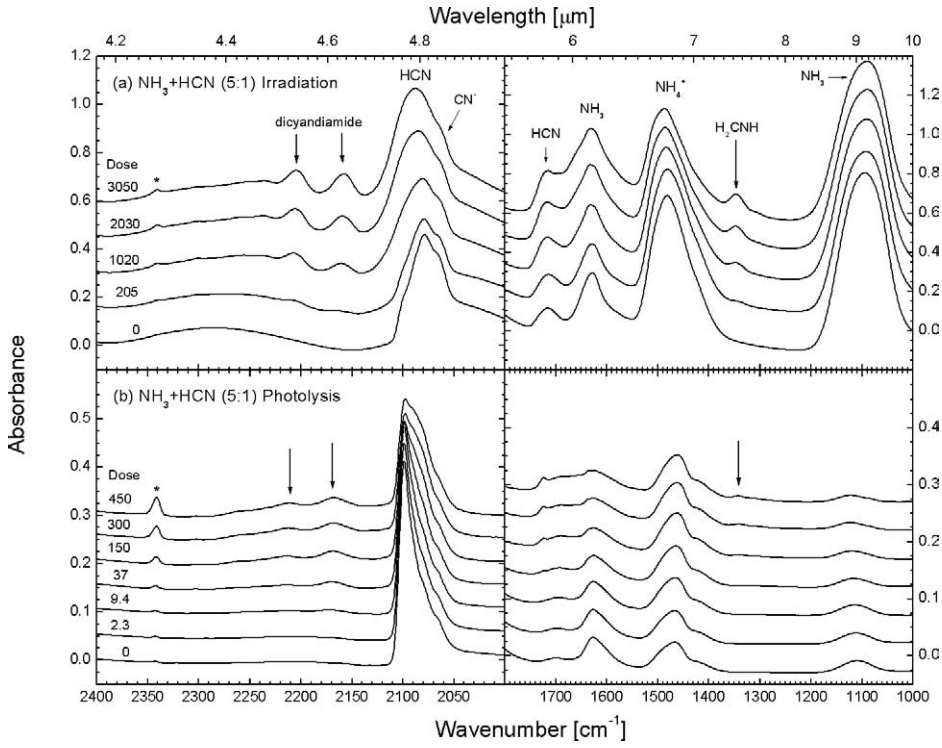

Fig. 6. IR spectra (left panels: 2400 to 2000 cm^{-1}; right panels: 1800–1000 cm^{-1}) of an $NH_3 + HCN$ (5:1) ice sample processed at 18 K by (a) irradiation (5.3 μm in thickness) and (b) photolysis (about 1 μm in thickness). Doses are in units of 10^{17} eV cm^{-2}. The feature due to the CO_2 impurity at 2342 cm^{-1} is labeled with an asterisk.

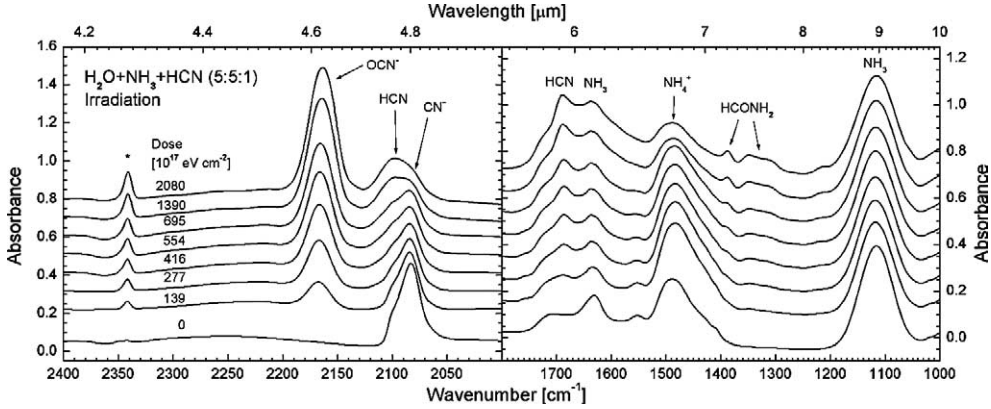

Fig. 7. IR spectra (left panel: 2400 to 2000 cm^{-1}; right panel: 1800–1000 cm^{-1}) of an $H_2O + NH_3 + HCN$ (5:5:1) ice sample processed at 18 K by irradiation. Spectra are labeled with the irradiation dose during the experiment (in units of 10^{17} eV cm^{-2}). The feature of CO_2 at 2342 cm^{-1} is labeled with an asterisk.

ences between the two processing techniques in this case as well.

Spectra of the ice sample over the course of the experiment are shown in Fig. 7. The NH_4^+ and CN^- features, at 1479 and 2080 cm^{-1}, respectively, were seen in the initial deposit at 18 K as in the $NH_3 + HCN$ (5:1) ice sample described previously. However, in contrast to the $NH_3 + HCN$ sample, no absorptions due to crystalline NH_4CN were obtained after annealing the $H_2O + NH_3 + HCN$ ice. The presence of H_2O seems to inhibit its formation. Some small amount of CO_2 is also present near 2342 cm^{-1} due to impurities in the original gas mixture, and this feature grows during processing due to the production of CO_2 from the ice mixture.

During proton irradiation, the feature of CN^- at 2080 cm^{-1} decreases with respect to that of HCN at 2100 cm^{-1}. The NH_4^+ feature at 1479 cm^{-1} also appears to weaken with irradiation as in the $NH_3 + HCN$ (5:1) sample. As in the $H_2O + HCN$ (5:1) ice sample, the OCN^- feature near 2160 cm^{-1} was observed, but features of isocyanic acid (HNCO) were absent near 2260 cm^{-1} (Fig. 7). If HNCO is formed by reactions between HCN and H_2O (as in the ammonia-free ice), it is rapidly neutralized by an acid-base reaction with the NH_3 in this sample to form ammonium

cyanate (NH_4OCN). This is evidenced by the growth of the OCN^- absorption feature near 2160 cm^{-1} during irradiation. (A comparison of the upper traces of Figs. 4b and 7 clearly demonstrates the role of NH_3 in driving the chemistry from HNCO to OCN^-.) The weakening of the NH_4^+ feature at 1479 cm^{-1} seems to contradict this idea, but recall that NH_4^+ is also present in the initial ice deposit, indicating that the NH_3 and HCN in the deposit react at 18 K to produce NH_4CN in the unirradiated ice sample (see Fig. 7). Our observation of a decreasing NH_4^+ absorption feature during irradiation may be explained if this initial NH_4CN is destroyed more rapidly by the irradiation than the NH_4OCN is produced. This is also consistent with the observation that the CN^- feature at 2080 cm^{-1} (also in the unirradiated ice spectrum) decreases with irradiation dose. The features of formamide ($HCONH_2$) are also seen near 1380 cm^{-1}.

As noted in previous experiments, the feature of HCN is seen to redshift and broaden with energy dose (Fig. 7), possibly due to the growth of an underlying feature of the CN^- anion, centered near 2080 cm^{-1}.

3.5. Formation/destruction rates

Rates of formation, G (in units of molecules per 100 eV), as measured from the evolution of the IR spectra of each experiment, are listed in Table 1. Values of G were calculated as described by Gerakines et al. (2000) and Gerakines and Moore (2001): from the slope of a line constrained to pass through the origin and fit to the low-energy-dose portion of the graph of column density (in molecules cm^{-2}) vs. total energy absorbed (in eV cm^{-2}), which typically displays a linear dependence of column density with energy dose. The listed error in each value of G represents the standard deviation in the ratio of column density to applied energy for the data points to which the slope was fitted.

Destruction rates for HCN as a result of energetic processing could not be accurately calculated in most cases, especially where both NH_3 and HCN were present. This is due to the overlapping spectral features of HCN and CN^-. Moreover, CN^- appears to be produced directly upon sample creation in some cases, so that features of HCN itself are not visible in the unprocessed ice spectra (e.g., the thick

Table 1

Sample composition	Species	Wavenumber [cm^{-1}]	Formation rates, G [molecules per 100 eV][a]	
			Irradiation	Photolysis[b]
Pure HCN				
	HCN	2100	-1.1 ± 0.5	-4.0 ± 0.4
	CN^-	2090	–	–
	CO_2 (impurity)	2342	–	–
	Unidentified	2217	–	–
	Unidentified	1455	–	–
	Unidentified	1079	–	–
$H_2O + HCN$ (5:1)				
	HCN[c]	2100	-1.0 ± 0.2	-1.27 ± 0.02
	CO_2[d]	2342	0.01 ± 0.006	0.037 ± 0.003
	HNCO[e]	2268	0.06 ± 0.01	0.045 ± 0.004
	OCN^-[f]	2169	$(1.2 \pm 0.4)/A_{2160}$	$(1.4 \pm 0.5)/A_{2160}$
	NH_4^+	1470	?[g]	–
	$HCONH_2$[f]	1386	$(0.14 \pm 0.03)/A_{1380+1330}$	?[g]
$NH_3 + HCN$ (5:1)				
	HCN	2100	?[h]	?[h]
	H_2CNH[f]	1347	$(0.07 \pm 0.01)/A_{1347}$	$(0.035 \pm 0.004)/A_{1347}$
	$NHC(NH_2)NHCN$	2205, 2159	0.34 ± 0.05	?[g]
$H_2O + NH_3 + HCN$ (5:5:1)				
	HCN	2100	?[h]	–
	OCN^-[f]	2160	$(2.4 \pm 0.2)/A_{2160}$	–
	NH_4^+[f]	1479	$(-1.2 \pm 0.3)/A_{1480}$[i]	–
	$HCONH_2$[f]	1380	$(0.20 \pm 0.04)/A_{1380+1330}$	–

[a] Negative values of G indicate destruction rates.
[b] Rates from photolysis experiments were determined assuming a total lamp photon flux of 5.3×10^{14} $cm^{-2}\,s^{-1}$ and an average photon energy of 7.9 eV.
[c] Assumes $A(HCN, 2092\ cm^{-1}) = 5.1 \times 10^{-18}$ cm molecule^{-1}.
[d] Assumes $A(CO_2, 2340\ cm^{-1}) = 7.6 \times 10^{-17}$ cm molecule^{-1}.
[e] Assumes $A(HNCO, 2260\ cm^{-1}) = 1.6 \times 10^{-16}$ cm molecule^{-1}.
[f] The absorption strength for this species is uncertain. G is obtained by inserting a value for A_ν, in units of 10^{-17} cm molecule^{-1}, for the strength of this absorption feature at wavenumber ν. See text.
[g] The lack of linear growth prevented the accurate measurement of G.
[h] Overlapping features of HCN and CN^- prevented accurate measurement of HCN destruction rates in this case.
[i] NH_4^+ is formed upon deposit. After the first dose of irradiation, it appears to increase in abundance, followed by a linear decrease for later irradiation doses at the rate listed. See text.

NH_3 + HCN and H_2O + NH_3 + HCN ice samples—see Figs. 6 and 7). For these ices, a large uncertainty in G results (on the order of 50%; see Table 1).

In the case of the H_2O + HCN samples, the rates of growth for the features of HNCO, CO_2, OCN^-, NH_4^+, and formamide ($HCONH_2$) were measured. For CO_2 and HNCO, values of G were calculated from the linear part of the curve of growth using the following absorption strengths: $A(CO_2, 2340\ cm^{-1}) = 7.6 \times 10^{-17}$ cm molecule^{-1} (Gerakines et al., 1995), $A(HNCO, 2260\ cm^{-1}) = 1.6 \times 10^{-16}$ cm molecule^{-1} (Lowenthal et al., 2002; for solid HNCO at 145 K).

Values of G for OCN^-, NH_4^+, and $HCONH_2$ cannot be absolutely determined, because accurate absorption strengths for these ice species are either unknown or deemed by us to be poorly constrained by the experimental data in the literature. In these cases, values of G in Table 1 are left in terms of the unknown absorption strengths, A, and readers are encouraged to use more certain values once they become published. For the purpose of comparison *in this discussion only*, we use of the following tentative estimates of A: for OCN^-, a commonly adopted value (e.g., Gibb et al., 2000) consistent with most nitriles in H_2O-dominated ices (e.g., Bernstein et al., 1997) is about 1×10^{-17} cm molecule^{-1}. This value, when combined with data from Table 1, results in a value of $G(OCN^-)$ of 1.2 ± 0.4 molecules per 100 eV for the H_2O + HCN (5:1) irradiation experiment and 1.4 ± 0.5 for the corresponding photolysis. For NH_4^+, Demyk et al. (1998) and Schutte and Khanna (2003) adopt values of about 4×10^{-17} cm molecule^{-1}. This leads to an estimate of $G(NH_4^+) = -0.3 \pm 0.1$ for its destruction in the H_2O + NH_3 + HCN (5:5:1) irradiation experiment (see Table 1). For solid formamide ($HCONH_2$), the strengths of its features at 1380 and 1330 cm^{-1} in ices are unknown.

For the NH_3 + HCN (5:1) ice samples, we have measured the rate of growth of the features at 2205 and 2159 cm^{-1} in order to calculate the formation rate of the presumed carrier of these features, dicyandiamide [NHC(NH_2)-NHCN]. Bernstein et al. (1997) measured the strength of these combined features to be $A(\text{dicyandiamide}, 2205 + 2159\ cm^{-1}) = 5.1 \times 10^{-18}$ cm molecule^{-1} in an H_2O ice at 20 K. Assuming this value is valid for an NH_3-dominated ice sample, and combining it with the slope of the linear part of the growth curve, we calculate $G = 0.34 \pm 0.05$ molecules per 100 eV for dicyandiamide for the irradiation experiments. For photolysis, there was no clear linear growth in these features of dicyandiamide, whose areas leveled off and remained approximately constant after only 16 min of photolysis (4.0×10^{18} eV cm^{-2}), and thus no accurate value of G could be obtained. Clear linear rates of growth were observed for the feature assigned to H_2CNH near 1347 cm^{-1} in each set of experiments. However, the strength of this feature is unknown. As described above for other products, the formation rates listed in Table 1 for H_2CNH are left in terms of the unknown strength of its feature.

In the H_2O + NH_3 + HCN (5:5:1) irradiation experiment, rates for OCN^-, NH_4^+, and $HCONH_2$ were determined, although not absolutely due to uncertainties in the strengths of the features. In comparison to the H_2O + HCN (5:1) irradiation experiment, the rate of OCN^- formation was a factor of two higher, while the rate of $HCONH_2$ formation was only increased by about 1.4 times.

3.6. Residues

The IR spectra of the room-temperature residues of the irradiated samples are shown in Fig. 8. The IR spectrum of "poly-HCN" as prepared by Khare et al. (1994) is also shown for comparison to the residues of the irradiated samples. The pure HCN residue spectrum below about 1500 cm^{-1} is also in reasonable agreement with that of HCN polymer as prepared by Matthews and Ludicky (1986) and published by Cruikshank et al. (1991), in their Fig. 2. No further chemical analyses have yet been performed on our residues (this is a future project), but we expect to find large organic molecules similar to those discussed by Khare et al. (1994).

4. Discussion

4.1. Comparisons of irradiation and photolysis experiments

In these experiments, it was found that energetic processing by 0.8-MeV proton irradiation and vacuum-UV photolysis of pure HCN, H_2O + HCN (5:1), NH_3 + HCN (5:1), and H_2O + NH_3 + HCN (5:5:1) ice mixtures at 18 K result in similar mid-infrared features and the same chemical products. A quantitative comparison of product formation rates and reactant destruction rates was complicated by the nature of the ice mixtures studied—specifically, the formation of NH_4CN upon deposit of the NH_3 + HCN ice mixtures (see Table 1 and Figs. 5 and 6) or the lack of a clear linear growth in the resulting infrared absorption features (e.g., the case of NH_4^+ in the H_2O + HCN irradiation experiment; see Table 1). Irradiation and photolysis production rates that were measured differed by up to a factor of 4 (see results of H_2O + HCN experiments in Table 1). For the case of pure HCN subjected to energetic processing, the rate of destruction due to UV photolysis was higher by about a factor of 4. While the rates do vary somewhat, the fact that the results of irradiation and photolysis are similar does imply that HCN-containing ice mixtures that undergo these different forms of processing in space (in the form of cosmic rays, the interstellar radiation field, Solar UV, or other types of radiation) will show similar chemistries.

Comparisons between the chemical effects of irradiation and vacuum-UV photolysis made here and previously by us (e.g., Gerakines et al., 2000, 2001), when examined together with high energy UV photolysis studies using 30 and 58 nm photons by Wu et al. (2003), point to the fact that the most

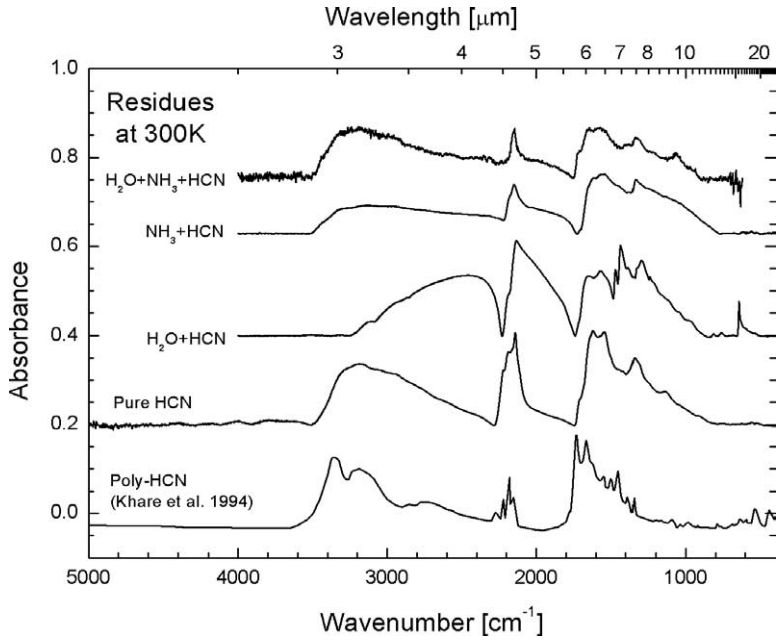

Fig. 8. IR spectra of residues remaining after ice sample irradiation and slow warm-up to 300 K. The spectrum of poly-HCN (tholin) from Khare et al. (1994) is shown for comparison.

important parameter in determining the outcome of these experiments is not the *nature* of the incident energy (photons or ions) but the *total energy dose* absorbed by the sample. However, experimental results do diverge when the reactants do not absorb uniformly over the energy range of the incident radiation, and in these cases the absolute energy of the radiation must also be taken into account. For instance, this is true of vacuum-UV photolysis experiments containing CO or N_2 ices. These molecules possess dissociation energies of 9.8 eV ($\lambda = 127$ nm) and 11 eV ($\lambda = 113$ nm), respectively, that lie beyond the primary spectral range of the UV lamp, but well below the energy of 0.8-MeV protons used in irradiation experiments (see Fig. 1 and the results of experiments by, for example, Gerakines and Moore, 2001; Hudson and Moore, 2002; Bernstein et al., 2003).

Ice sample thickness must also be taken into account when examining differences in photolysis and irradiation effects. As stated in Section 2, penetration depths for energetic particles are 100 times greater than those for UV photons. In the simplified case of a macroscopic ice with no weathering or diffusion effects, only the top few microns of an ice will be processed by UV, while up to a few millimeters may be processed by irradiation. In our experiments, we have not examined the effects of ice thickness on our results, but only the chemical changes induced by each form of processing. Some effects of ice thickness on radiation-induced chemistry were examined previously by Gerakines et al. (2000).

4.2. Astrophysical implications

What do these experiments tell us about interstellar HCN, the source of cometary HCN, or the stability of HCN in H_2O-dominated ices? As demonstrated in our $H_2O + HCN$ and $H_2O + NH_3 + HCN$ ice mixture experiments, HCN will quickly be converted into HNCO, NH_4^+, and OCN^- by radiation in ice environments dominated by H_2O (e.g., the ISM, comets). Both NH_4^+ and OCN^- are suspected to be present in interstellar ices and HNCO is detected as a gas-phase species in both interstellar sources and in comets (e.g., Gibb et al., 2000; Schutte and Khanna, 2003). The detection of any condensed-phase HNCO in interstellar ices would suggest the absence of NH_3 since, as shown in our experiments, acid-base reactions will convert NH_3 to other species, even at very low temperatures. The identification of OCN^- in interstellar ices along certain lines of sight suggests that acid-base reactions have indeed occurred there, and that HCN or NH_3 would be unlikely to be found in the ices in those environments.

Several arguments support the idea that HCN is a parent volatile in comets, although for Hale–Bopp, a probable, additional extended source was observed. Photodissociation of HCN in the comae of comets is the major source of CN emissions, even though an extra, extended source is required to explain the observed distributions and abundances in some comets. HCN is seen in the emission of cometary comae with a relative abundance (HCN/H_2O) of about 0.4% (for Comet Hale–Bopp; see Magee-Sauer et al., 1999, or Bockelée-Morvan et al., 2000). This cometary HCN abundance is well below the detection limit for modern interstellar ice observations, which thus far have not been shown to contain solid HCN absorption features at all.

However, HCN is presumed to be a component of interstellar ices based on its abundance in the gas-phase of interstellar clouds. Studies of gas-phase interstellar HCN reveal that its column density is on the order of 10^{15} to 10^{16} cm^{-2} (10^{-7} to 10^{-6} relative to H_2), and the observed increase of

the HCN gas abundance with increasing temperature does seem to indicate a relationship with interstellar ices (see the study by Lahuis and van Dishoeck, 2000). Therefore, it is not out-of-bounds to suggest that cometary HCN is interstellar in origin. However, problems with this explanation remain, such as the fact that cold interstellar clouds have large gas-phase HNC/HCN ratios, whereas the cometary HNC/HCN abundance ratio varies with production rate and heliocentric distance (see Rodgers and Charnley, 2001).

Reconciling cometary observations of both HCN and its isomer HNC requires an extended source in addition to any nuclear source for HNC. Possible extended sources include the decomposition of small organic molecules, such as H_2CNH or HNCO, or larger molecules, such as HCN polymers (Rodgers and Charnley, 2001). The source of these possible organic molecules could come from processed interstellar ices. We have shown that H_2CNH and HNCO are products formed when $NH_3 + HCN$ and $H_2O + HCN$ ices, respectively, are either photolyzed or irradiated. Similarly, residues from our irradiated ice mixtures containing HCN have IR spectra very similar to poly-HCN and may contain many of the same large organic molecules.

We have also shown that HCN, in the presence of large quantities of NH_3, is very easily converted into NH_4CN, even at 18 K, or into NH_4OCN in the presence of H_2O. It is also worth noting that these experiments are the first to show that NH_3 is not a necessary starting ingredient in order to create OCN^- in astrophysical ices. This might explain why HCN is not seen in interstellar ices—our experiments show that energetic processing would quickly convert interstellar HCN to OCN^- (which is a large component of interstellar ices) in H_2O-dominated ices, even without NH_3. Moreover, NH_4CN and NH_4OCN are salts that are less volatile than H_2O, and therefore they could be possible extended sources of HCN in comets. Additional studies of these molecular species embedded in an H_2O-dominated cometary ice analog, involving energetic processing or thermal evaporation, may reveal interesting results that are related to HCN and its evolution in comets.

Finally, it is worth mentioning that although the experiments described here were done around 18 K, the chemistry observed also will likely also apply at much higher temperatures such as the 90 K or so at Titan. Products such as NH_4^+, CN^-, OCN^-, and polymeric material are stable up to room temperature (300 K).

Acknowledgments

Steve Brown, Scott Kniffin, and Claude Smith from NASA/GSFC's Radiation Effects Facility are thanked for help with the irradiations. P.A.G. thanks reviewers Max Bernstein and Robert Carlson for their many useful comments. These experiments were performed while P.A.G. held a NRC-NAS/NASA-GSFC research associateship.

References

Bernstein, M.P., Sandford, S.A., Allamandola, L.J., 1997. The infrared spectra of nitriles and related compounds frozen in Ar and H_2O. Astrophys. J. 476, 932–942.

Bernstein, M.P., Dworkin, J.P., Sandford, S.A., Cooper, G.W., Allamandola, L.J., 2002. Racemic amino acids from the ultraviolet photolysis of interstellar ice analogues. Nature 416, 401–403.

Bernstein, M.P., Moore, M.H., Elsila, J.E., Sandford, S.A., Allamandola, L.J., Zare, R.N., 2003. Side group addition to the polycyclic aromatic hydrocarbon coronene by proton irradiation in cosmic ice analogs. Astrophys. J. 582, L25–L29.

Bockelée-Morvan, D., Padman, R., Davies, J.K., Crovisier, J., 1994. Observations of submillimetre lines of CH_3OH, HCN, and H_2CO in Comet P/Swift–Tuttle with the James Clerk Maxwell Telescope. Planet. Space Sci. 42, 655–662.

Bockelée-Morvan, D., 16 colleagues, 2000. New molecules found in Comet C/1995 O1 (Hale–Bopp) investigating the link between cometary and interstellar material. Astron. Astrophys. 353, 1101–1114.

Boonman, A.M.S., Stark, R., van der Tak, F.F.S., van Dishoeck, E.F., van der Wal, P.B., Schäfer, F., de Lange, G., Laauwen, W.M., 2001. Highly abundant HCN in the inner hot envelope of GL 2591: probing the birth of a hot core? Astrophys. J. 553, L63–L67.

Büchler, H., Büchler, R.E., Cooper, R., 1976. Pulse radiolysis of aqueous cyanide solutions. Kinetics of the transient OH and H adducts and subsequent rearrangements. J. Phys. Chem. 80, 1549–1553.

Chyba, C.F., Owen, T.C., Ip, W.-H., 1994. Impact delivery of volatiles and organic molecules to Earth. In: Gehrels, T. (Ed.), Hazards Due to Comets and Asteroids. Univ. of Arizona Press, Tucson, pp. 9–59.

Clutter, D.R., Thompson, W.E., 1969. Infrared spectroscopic study of polycrystalline NH_4CN. J. Chem. Phys. 51, 153–159.

Cottin, H., Moore, M.H., Bénilan, Y., 2003. Photodestruction of relevant interstellar molecules in ice mixtures. Astrophys. J. 590, 874–881.

Cruikshank, D.P., Allamandola, L.J., Hartmann, W.K., Tholen, D.J., Brown, R.H., Matthews, C.N., Bell, J.F., 1991. Solid C≡N bearing material on outer Solar System bodies. Icarus 94, 345–353.

Demyk, K., Dartois, E., d'Hendecourt, L., Jourdain de Muizon, M., Heras, A.M., Breitfellner, M., 1998. Laboratory identification of the 4.62 μm solid-state absorption band in the ISO–SWS spectrum of RAFGL 7009S. Astron. Astrophys. 339, 553–560.

Draganić, I., Draganić, Z., Petković, Lj., Nikolić, A., 1973. The radiation chemistry of aqueous solutions of simple RCN compounds. J. Am. Chem. Soc. 95, 7193–7199.

Dressler, K., Schnepp, O., 1960. Absorption spectra of solid methane, ammonia, and ice in the vacuum ultraviolet. J. Chem. Phys. 33, 270–274.

Evans, R.A., Lorenčak, P., Ha, T.-K., Wentrup, C., 1991. HCN dimers: iminoacetonitrile and *N*-cyano-methanimine. J. Am. Chem. Soc. 113, 7261–7276.

Gerakines, P.A., Moore, M.H., 2001. Carbon suboxide in astrophysical ice analogs. Icarus 154, 372–380.

Gerakines, P.A., Schutte, W.A., Greenberg, J.M., van Dishoeck, E.F., 1995. The infrared band strengths of H_2O, CO, and CO_2 in laboratory simulations of astrophysical ice mixtures. Astron. Astrophys. 296, 810–818.

Gerakines, P.A., Schutte, W.A., Ehrenfreund, P., 1996. Ultraviolet processing of interstellar ice analogs. I. Pure ices. Astron. Astrophys. 312, 289–305.

Gerakines, P.A., Moore, M.H., Hudson, R.L., 2000. Carbonic acid production in $H_2O + CO_2$ ices—UV photolysis vs. proton bombardment. Astron. Astrophys. 357, 793–800.

Gerakines, P.A., Moore, M.H., Hudson, R.L., 2001. Energetic processing of laboratory ice analogs: UV photolysis versus ion bombardment. J. Geophys. Res. 106 (E12), 33381–33385.

Gibb, E.L., Whittet, D.C.B., Schutte, W.A., Boogert, A.C.A., Chiar, J.E., Gerakines, P.A., Keane, J.V., Tielens, A.G.G.M., van Dishoeck, E.F.,

Kerkhof, O., 2000. An inventory of interstellar ices toward the embedded protostar W33 A. Astrophys. J. 536, 347–356.

Gibb, E.L., Whittet, D.C.B., Chiar, J.E., 2001. Searching for ammonia in grain mantles toward massive young stellar objects. Astrophys. J. 558, 702–716.

Hudson, R.L., Moore, M.H., 1995. Far-IR spectral changes accompanying proton irradiation of solids of astrochemical interest. Radiat. Phys. Chem. 45, 779–789.

Hudson, R.L., Moore, M.H., 2002. The N_3 radical as a discriminator between ion-irradiated and UV-photolyzed astronomical ices. Astrophys. J. 568, 1095–1099.

Hudson, R.L., Moore, M.H., Gerakines, P.A., 2001. The formation of cyanate ion (OCN–) in interstellar ice analogs. Astrophys. J. 550, 1140–1150.

Ip, W.-H., 11 colleagues, 1990. IMS measurements of the production rate of hydrogen cyanide in the coma of Comet Halley. Ann. Geophys. 8, 319–325.

Jacox, M.E., Milligan, D.E., 1975. The infrared spectrum of methylenimine. J. Mol. Spec. 56, 333–356.

Khanna, R.K., Lowenthal, M.S., Ammon, H.L., Moore, M.H., 2002. Molecular structure and infrared spectrum of solid amino formate (HCO_2NH_2): relevance to interstellar ices. Astrophys. J. Suppl. Ser. 140, 457–464.

Khare, B.N., Sagan, C., Thompson, W.R., Arakawa, E.T., Meisse, C., Tuminello, P.S., 1994. Optical properties of poly-HCN and their astronomical applications. Can. J. Chem. 72, 678–694.

Kissel, J., 1986. The Giotto particulate impact analyzer. In: The Giotto Mission—Its Scientific Investigations. In: ESA SP, vol. 1077, pp. 67–68.

Lahuis, F., van Dishoeck, E.F., 2000. ISO–SWS spectroscopy of gas-phase C_2H_2 and HCN toward massive young stellar objects. Astron. Astrophys. 355, 699–712.

Lowenthal, M.S., Khanna, R.K., Moore, M.H., 2002. Infrared spectrum of solid isocyanic acid (HNCO): vibrational assignments and integrated band intensities. Spectrochim. Acta A 58, 73–78.

Magee-Sauer, K., Mumma, M.J., DiSanti, M.A., DelloRusso, N., Rettig, T.W., 1999. Infrared spectroscopy of the ν_3 band of hydrogen cyanide in Comet C/1995 O1 Hale–Bopp. Icarus 142, 498–508.

Matthews, C.N., Ludicky, R., 1986. The dark nucleus of Comet Halley: hydrogen cyanide polymers. In: 20th ESLAB Symposium, Exploration of Halley's Comet. In: ESA SP, vol. 250, pp. 273–277.

Morgan, H.W., Staats, P.A., Goldstein, J.H., 1957. Infrared spectra of $N^{15}H_3$ and $N^{15}H_4^+$. J. Chem. Phys. 27, 1212–1213.

Mumma, M.J., Weissman, P.R., Stern, S.A., 1993. Comets and the origin of the Solar System: reading the Rosetta stone. In: Levy, E.H., Lunine, J.I. (Eds.), Protostars and Planets III. Univ. of Arizona Press, Tucson, pp. 1177–1252.

Negrón-Mendoza, A., Draganić, Z.D., Navarro-González, R., Draganić, I.G., 1983. Aldehydes, ketones, and carboxylic acids formed radiolytically in aqueous solutions of cyanides and simple nitriles. Rad. Res. 95, 248–261.

Oro, J., Mills, T., Lazcano, A., 1992. Comets and the formation of biochemical compounds on the primitive Earth—a review. Origins Life 21, 267–277.

Rettig, T.W., Tegler, S.C., Pasto, D.J., Mumma, M.J., 1992. Comet outbursts and polymers of HCN. Astrophys. J. 398, 293–298.

Rodgers, S.D., Charnley, S.B., 2001. On the origin of HCN in Comet Lee. Mon. Not. R. Astron. Soc. 323, 84–92.

Schutte, W.A., Khanna, R.K., 2003. Origin of the 6.85 μm band near young stellar objects: the ammonium ion revisited. Astron. Astrophys. 398, 1049–1062.

Snyder, L.E., Buhl, D., 1971. Observations of radio emission from interstellar hydrogen cyanide. Astrophys. J. 163, L47–L52.

Wu, C.Y.R., Judge, D.L., Cheng, B.-M., Yih, T.-S., Lee, C.S., Ip, W.H., 2003. Extreme ultraviolet photolysis of CO_2–H_2O mixed ices at 10 K. J. Geophys. Res. 108 (E4), 5032. doi:10.1029/2002JE001932.